

## Famotidine as Urokinase Inhibitor in Anaphylactic Shock

Claudiu N Lungu\*

Department of Chemistry, Faculty of Chemistry and Chemical Engineering, Babes-Bolyai University, 400028 Cluj, Romania

## \*Corresponding author

Claudiu N Lungu, Department of Chemistry, Faculty of Chemistry and Chemical Engineering, Babes-Bolyai University, 400028 Cluj, Romania; E-mail: lunguclaudiu5555@gmail.com

Submitted: 03 Feb 2018; Accepted: 12 Feb 2018; Published: 10 Mar 2018

## Abstract

A QSAR study was performed on a series of naphthalene cyclohexane amines derivate with experimentally determine constant of inhibition ( $K_i$ ) in order to indentify a potent human urokinase inhibitor. A QSAR model was build using artificial neural networks (ANN). Model was used for screening of compounds with potent urokinase inhibitory properties and to compute  $K_i$  of resulted screening compounds. Compound with best  $K_i$  was chosen for discussion. An induced fit docking (protein - ligand) and a protein-protein docking were used in results discussion. A isoquinoline-diol base derivate (Famotidione) resulted to have urokinase inhibitory properties.

**Keywords:** Urokinase, Famotidine, QSAR, Virtual Screening, Artificial Neural Networks, Variance Inflation Factor

## Introduction

Urokinase is a serine protease present in humans' urine, blood and in extracellular matrix of many tissues. Urokinase is a 411 residue protein with three domains: the serine protease domain, the kringle domain and growth factor domain. It is synthesizing in zymogen form and activated by proteolytic cleavage between Lys 158 and Ile 159. Urokinase catalyzed the reaction of transforming plasminogen into plasmin. Urokinase has endogen inhibitors, most important being the serpins plasminogen activator inhibitor1 (PAI 1) and plasminogen activator inhibitor 2(PAI2) which are irreversible inhibitors [1,2]. Urokinase, Streptokinase and plasminogen activator respectively are alternatives to surgery for recanalizing thrombosed vessels or vascular prostheses. Anaphylactoid reactions are identical to anaphylactic reactions in their clinical presentation, but the former occurs without participation of immunoglobulin E antibodies or an inciting allergen. It is believed that urokinase directly stimulates mast cells and basophils to release the chemical mediators of inflammation.

The symptoms observed during this type of reaction result from release of histamine and other substances (e.g., leukotrienes, prostaglandins, kinins, and serotonin) from mast cells and basophils. Histamine then binds to H1 and H2 receptors on cells of the cardiovascular system, extra vascular smooth muscle (e.g., bronchial tree), and exocrine glands (e.g., lacrimal, bronchial, salivary, and gastric secretory cells) [3]. Histamine and serotonin stimulate the peripheral microvasculature causing vasodilation and vascular permeability, which can lead to hypotension, tachycardia, and shock. In the lungs bronchial smooth muscle spasm, mucosal edema, and mucus plugging can cause severe respiratory compromise.

Prophylaxis is realized using acetaminophen orally, intravenous diphenhydramine hydrochloride - a H<sub>1</sub> inhibitor. The possibility of using H<sub>2</sub> inhibitors was also suggested based on clinical observation [4]. In this respect a potent urokinase inhibitor is to be found.

## Methods

In order to developed a QSAR model of urokinase inhibitors, with further used in virtual screening of novel urokinase inhibitors, a data set of compounds with experimentally determine constant of inhibition ( $K_i$ ) on urokinase was chosen [5]. Data were curated in order to have a correspondent distinct value of  $K_i$  for a distinct molecule. Also the 3D structures were energetically minimized, partial charges corrected; naming issues resolved. Furthermore three molecules containing Br were removed from the data set due to failure in computing partial charges. Data set was divided into a training set used to build the model and a test set used to externally validate the model. Data were split using a randomized algorithm in a training set (21 compounds) used to build the model and a test set (21 compounds) used to test the model. Target variable was set as inhibition constant ( $K_i$ ).

A number of chemical descriptors were used: H, C, N, O, P, S atoms, molecular weight (MW), total number of atoms, number of heavy atoms, number of rotational bounds, number of hydrogen donor groups (HD), number of hydrogen accepting groups (HA), number of rings, minimal distance between two hydrogen donor groups, maximal distance between two hydrogen donor groups, minimal distance between two hydrogen accepting groups, maximal distance between two hydrogen accepting groups, aromaticity (Aro). A future selection algorithm was used to select proper descriptors. Also descriptors were evaluated using tolerance (T) and variance inflation factor (VIF). In order to evaluate tolerance and VIF  $r^2$  of each descriptor in respect to all others was computed. Artificial neural

networks (ANN) regression was used in building the model due to failure of multiple linear regression method (MLR) in predicting the target variable ( $r^2 < 0.7$ ) [6,7]. ANN attributes were a neurons incl. bias –input-hidden layer-output were 11,4,1, max epoch was 1000, general learning rate 0.3, output layer learning rate used was back propagation method was 0.3, initial weight range was 0.5 respectively. Structures composing the ANN model were arrange based on similarity score composed on best  $K_i$  and best correlation with the ANN model. Ligand molecule accordingly to best  $K_i$  was chosen as a template and a similarity screening was performed on a commercially available data base [8]. QSAR model previously obtained was applied on the retrieved set of molecules in order to compute the  $K_i$ . A comparative docking study was performed on ligand data set on endogen urokinase inhibitors API-1 and API 2. In first docking study ligands were docked on urokinase crystallographic structure with the PDB id 1C5Y. Auto Dock 4.2 software was used for docking procedure [9]. Docking site was retrieved from literature and its precise coordinates detected computationally where: x 8.84Å, y 3.18Å, z 29.94Å with a radius of 15Å. A protein-protein docking study was performed with urokinase as a target and API-1 and API-2 as ligands.

## Results and Discussion

Descriptors proposed for regression model building using ANN are represented in Table 1. Descriptor analysis suggested that Andrews's charges, minimal distance between a hydrogen donor an acceptor group, minimal distance between a hydrogen donor group and a radical group and aromaticity contribute with relevant information to model. Also number of S atoms although there are only three sulfur containing compounds is significant. Hydrogen number and the total number of atoms of each compound, accordingly to T and VIF do not contribute with significant information and were not used in building the model. Lastly for 42 compounds 8 descriptors were used.

**Table 1: Descriptors proposed for model building. Pearson correlation square coefficient ( $r^2$ ), tolerance (T), variance inflation factor (VIF) are computed**

Number	Descriptor	$r^2$	T	VIF
1	H	0.994282	0,005718	0,005718
2	Atoms	0.994584	0,005416	0,005416
3	Rings	0.948783	0,051217	0,051217
4	Aro	0.899219	0,100781	0,100781
5	Csp3	0.98473	0,01527	0,01527
6	S	0.527008	0,472992	0,472992
7	Andrews	0.87286	0,12714	0,12714
8	HD-HA-Min	0.78283	0,21717	0,21717
9	HD-R-Min	0.822778	0,177222	0,177222
10	Wiener	0.98303	0,01697	0,01697

**Table 2: Observed and predicted inhibition constants. Ki-observed inhibition constant, Kip –predicted inhibition constant (nM)**

Nr	Compound	Ki	Kip
1	<chem>O=S(=O)(C)N([CH1])[N]C=C1[c]([cH2])[c]3[cH][c]([c](n)[nH])[cH][cH][c]3[cH][c]2c(=O)[nH]=c4[cH][cH][cH][cH]4</chem>	769	-1445.21
2	<chem>[nH][c](n)[c]([cH1])[cH][cH][c]([cH2])[c]1[cH][cH][c]2OC(C)C</chem>	7280	6321.44
3	<chem>C#CCN(C)C(=O)c(cc1)cc(c12)nc(N)cc2</chem>	100000	102379
4	<chem>[nH][c](n)[c]([cH1])[cH][cH][c]([cH2])[c]1[cH][cH][c]2C3CC3[c]([cH][c]54)[cH][cH][c]5CCN(C)C4C6CCC6</chem>	42	2237.42
5	<chem>N#CCN(C)C(=O)c(cc1)cc(c12)nc(N)cc2</chem>	100000	99954.9
6	<chem>[nH][c](n)[c]([cH1])[cH][cH][c]([cH2])[c]1[cH][cH][c]2C=C[c]([cH][c]43)[cH][cH][c]4CCN(C)C3C5CCCC5</chem>	223	1708.24
7	<chem>[nH][c](n)[c]1[cH][cH][c]2[cH][cH][cH][c]c(=NH2)[c]2[cH]1</chem>	4500	-1655.29
8	<chem>[O][C](OC)[NH]=c([cH1])[c]2[cH][c]([c](n)[nH])[cH][cH][c]2[cH][c]1c(=O)[nH]=c3[cH][cH][cH][cH]3</chem>	18	7121.53
9	<chem>COC(=O)Nc(cc1)cc(c12)ccc(n2)/C(=N/[H])N</chem>	50000	49577.9
10	<chem>O=c([nH]=c1[cH][c](OC)[cH][c]([cH1])OC(C)C)[c]2[cH][c]3[cH][cH][c]([c](n)[nH])[cH][c]3[cH][cH]2</chem>	33	-1337.16
11	<chem>[H]N=C(\N)NC(=O)c1ccc(Cl)c(c1)S(=O)(=O)N</chem>	100000	87820
12	<chem>[nH][c](n)[c]([cH1])[cH][cH][c]([cH2])[c]1[c](C=CC3CC3)[cH][c]2C4CC4[c]([cH][cH]5)[cH][c]6[c]5CCN(C)C6C(C)C</chem>	9	570.307
13	<chem>[nH][c](n)[c]([cH1])[cH][cH][c]([cH2])[c]1[c](OC)[cH][c]2C3CC3[c]4[cH][c]5C(C(C)C)N(C)CC[c]5[cH][cH]4</chem>	94	3595.16
14	<chem>O=c(n)[c]1[cH][cH][cH][cH][c]1)[c]2[cH][cH][c]3[cH][c]([c](n)[nH])[cH][cH][c]3[cH]2</chem>	628	275.133
15	<chem>O=c([nH]=c1[cH][cH][cH][cH][c]1)[c]([cH2])[cH][c]3[cH][cH][c]([c](n)[nH])n)[cH][c]3[c]2[c]4[n][cH][cH][cH][n]4</chem>	7850	-3983.96
16	<chem>[nH][c](n)[c]1[cH][cH][c]2[cH][cH][cH][c]c(=NH2)[c]2[cH]1</chem>	450	21109.9
17	<chem>O=C([NH]=c1[cH][cH][cH][cH][c]1)[NH]=c2[cH][c]3[cH][cH][c]([c](n)[nH])[cH][c]3[cH][cH]2</chem>	610	1092.17
18	<chem>[nH][c](n)[c]([cH1])[cH][cH][c]([cH2])[c]1[cH][cH][c]2C3OC3[c]4[cH][cH][cH][cH][c]4</chem>	610	-5327.77
19	<chem>c1c(N)ccc(c12)cccc2</chem>	30000	20226.4
20	<chem>[nH][c](n)[c]([cH1])[cH][cH][c]([cH2])[c]1[cH][cH][c]2C3CC3[c]([cH][c]54)[cH][cH][c]5CCN(C)C4[c]6[cH][cH][cH][n][cH]6</chem>	1250	-4520.08
21	<chem>[nH][c](n)[c]([cH1])[cH][cH][c]([cH2])[c]1[c](C=CCOC)[cH][c]2C3CC3[c]4[cH][c]5C(C(C)C)N(C)CC[c]5[cH][cH]4</chem>	21	2300.85

Obtained model equation was  $y = 53.4084 + 0.956756 * K_i$ . Observed Pearson correlation square ( $r^2$ ) was 0.9614 and cross validated square CC ( $q^2$ ) was 0.960921 respectively. Correlation between  $K_i$  used in the model training and  $K_i$  prediction of training set is shown in figure 1 and Table 2

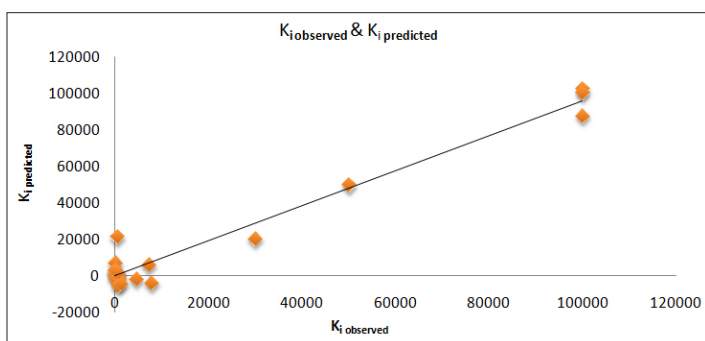


**Figure 1:** Scatter plot of inhibition constant ( $K_i$ ) observed versus  $K_i$  predicted by the ANN model. Scatter plot displays a regression where the majority of values is located at boundary of regression line. Moderate data is interpreted by relatively reduce size of compound set. Similarity ranking retrieved compound with molecular formula  $C_{21}H_{22}N_5O_3$  ( $K_i=0.9$ ) that is represented in figure below.

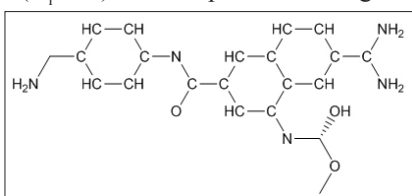


**Figure 2:** Ligand 9 hexahydro-naphthalen-methanol. This compound was used as a template for a shape screening using in a 3D chemical compound data base. Structures retrieved were purin-tione, isoquinoline-carboxilate, isoquinoli-benzamida, sulfanoylpropanimidamide (Famotidine), benzodiazepine, nitrobenzamide, pyrrolidine-carboxamide, enamide, metoxy-benzamide, isoquinoline and hexanamide respectively, listed in the table below and dranked accordingly to shape similarity and conformational energy. Also in Table 3 drugs like properties are estimated using Lipinski's rule of five.

**Table 3:** Compounds resulted after a shape screening classified after conformational energy and shape ranking. In the third column Lipinski's rule of five is calculated for all compounds assessing the lead like properties: from left to right molecular mass in Daltons, number of H donor groups, and number of H accepting groups, number of rotatable bounds.

	Molecule	Conformational energy (kcal/ mol)	Shape ranking
1	<chem>n1c(N)[nH]c(=S)c(c12)ncn2[C@@H]3O[C@@H](CO)[C@H](O)[C@H]3O</chem>	23.949	0.427
2	<chem>COC(=O)[C@@H]([C@@H](O)CC1)[C@H]([C@@H]12)C[C@H]3c4c(CCN3C2)c5c([nH]4)cccc5</chem>	205.160	0.426
3	<chem>c1cc(O)c(O2)c3c1C[C@@H](N(CC4)CC5CC5)[C@]6(O)CC[C@H]([C@H]2)[C@@]346)NC(=O)c7cccc7</chem>	167.780	0.419
4	<chem>O=S(=O)(N)/N=C(N)CCSCc1nc(sc1)N=C(N)N</chem>	310.354	0.417
5	<chem>c1c(O)c(O)c(Cl)c(c12)CC[NH2+] C[C@@H]2c3cccc3</chem>	104.847	0.416

6	<chem>c1cc(O)c(O2)c3c1C[C@@H](N(CC4)CC5CC5)[C@]6(O)CC[C@H]([C@H]2)[C@@]346)NC(=O)c7cc([N+](=O)[O-])ccc7</chem>	213.184	0.414
7	<chem>C1CC[C@@H](C(=O)N)N1C(=O)[C@H](Cc2[nH]cnc2)NC(=O)[C@@H]3CCCC(=O)C3</chem>	959.662	0.414
8	<chem>CCCC[C@@H](O)\C=C\[C@@H]([C@H](O)C[C@H]1O)[C@H]1C/C=C/CCCC(=O)N</chem>	112.731	0.408
9	<chem>COc1cccc(c1)C(=O)N[C@@H](CC2)[C@H]3Oc(c(O)cc4)c5c4C[C@@H]([C@@]2([C@@]356)O)N(CC6)CC7CC7</chem>	247.853	0.404
10	<chem>CC(=O)O[C@@H](CC1)[C@@H]2Oc(c(cc3)OC(=O)C)c4c3C[C@H]([C@H]1)[C@]245)N(C)CC5</chem>	3740.653	0.400
11	<chem>c1ccccc1C[C@@H](N)C(=O)N[C@H](Cc2cccc2)C(=O)N[C@H](CCCC)C(=O)N[C@@H](C(=O)N)CCC N=C(N)N</chem>	217.546	217.546

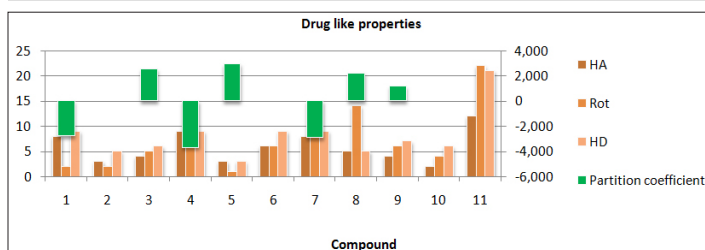


**Figure 3:** Combo cluster column plot representing drug like properties according to Lipinski's rule. For molecular mass values see supplemental materials.

Inhibitory constants calculated for compounds in table 2 using the ANN model are shown in figure 4

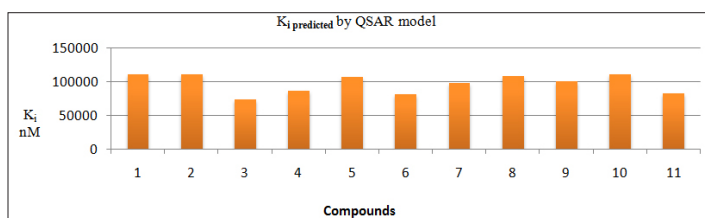


**Figure 4:** Cluster column plot representing  $K_{i \text{ predicted}}$  for compounds resulted after screening, using QSAR model. Compound 9 (figure 2) docked with urokinase is shown below (figure 5)

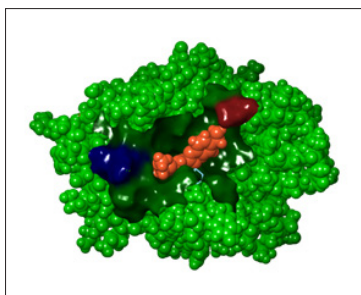
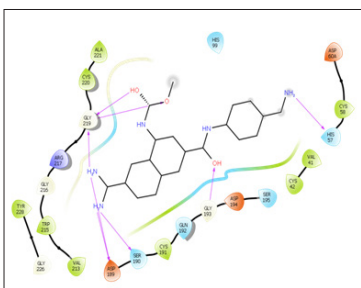
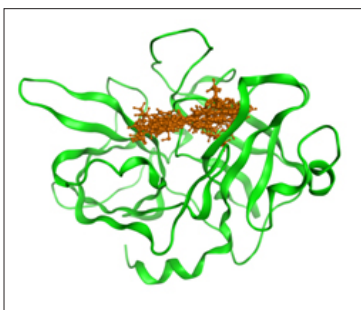


**Figure 5**

**a.** Ligand with best  $K_i$  docked with urokinase. Urokinase represented as space filling colored in green, compound 9 in space filling colored orange. Binding site cavity represented as space filling colored orange. Binding site cavity represented as space filling colored orange, colored by potential charges: red –positive charges, blue - negative charges.



**b.** Ligand interaction with Aa at binding pocket are shown hydrogen bonds are formed between NH<sub>2</sub> groups- His 57, Ser 190, Asp 189, Gly 219, OH groups –Gly 193, Gly 219 and O – Gly219.



**c.** Ligand 9 at binding site in various conformations, urokinase showed as green ribbons, compound 9 poses represented as sticks gold orange.

Accuracy of docking is shown in figure 5c. All poses are located at the same binding site, relatively in same position. Energy of each pose is represented in figure 6. All 9 poses were considered to their low favorable complex energies.

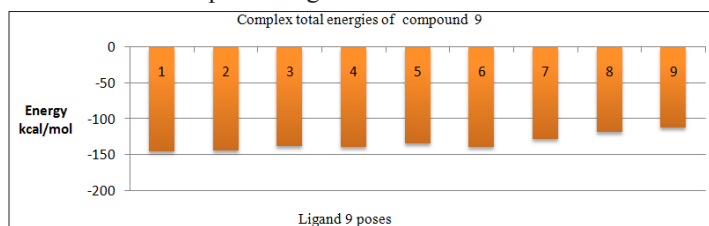


**Figure 6:** Cluster column plot of complex total energies between urokinase and ligand 9 poses.

Ligand 3 resulted from the shape screening and predicted by ANN model with a  $K_i$  of 73281.7 nM was docked with urokinase. Results are shown in figure 7

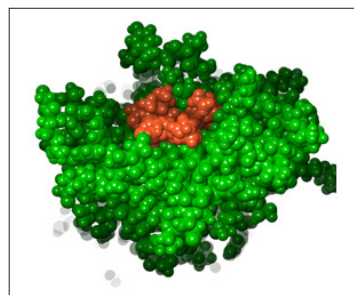
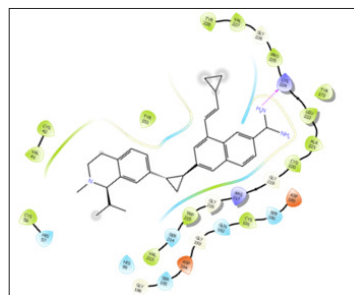


**Figure 7**

**a.** Ligand3 (with best  $K_i$  Predicted) docked with urokinase. Urokinase represented as space filling colored in green, compound 3 in space filling colored orange.



**b.** Ligand interaction with Aa at binding pocket are shown hydrogen bonds are formed between NH<sub>2</sub> group- Lys 224

5 possible poses were retained from ligand 3 after docking with urokinase. Complex energies observed were almost half of those of compound 9 (figure 8)

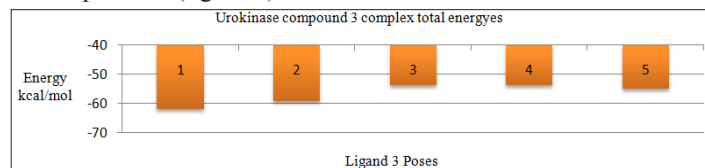


**Figure 8:** Complex total energies between urokinase and ligand3 poses.

In order to compare complex energies and to correlate found values with  $K_i$  a protein-protein docking was performed between urokinase and his endogenous inhibitor API-1.

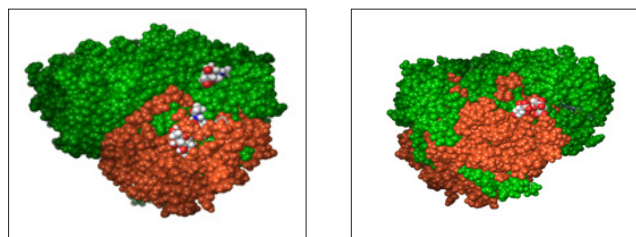


**Figure 9:** API -1 docked with Urokinase. Back and front view rotated around y axis. Space filling: APA1 represented in orange and Urokinase in green, NAG 952,953,954, ACE 900 represented as atom color- C grey, O red, N blue.

Docking energies were retained for 50 energetically achievable poses (poses with negative values for total energy). Finest energy observed after docking was 54.55kcal/mol. All energies are shown in figure 10.

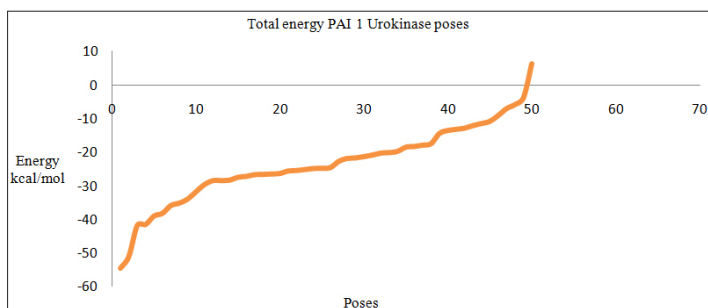


**Figure 10:** Total energy of PAI 1 Urokinase poses.

## Discussion

The  $K_i$  of an inhibitor (equivalent to  $K_d$ ) is, all by itself, an excellent way of stating the potency of an inhibitor and of comparing inhibitors to each other. Frequently, one measures the  $IC_{50}$  rather than the  $K_i$ , but that is equally useful because the  $IC_{50}$  is usually directly proportional to the  $K_i$ . The Cheng-Prusoff equation expresses this proportionality. Clearly, the compound must be an effective inhibitor. But it needs to have some other properties: it needs to be able to travel from the point of administration to the target tissue, and it needs to be harmless (or nearly so) to the patient on its way to its target. So compounds that are inadequately bio available - that is, having insufficient ability to get to the target tissue are poor drugs even if they are good inhibitors. Furthermore, compounds that are highly toxic are poor drugs. Often compounds that have been designed via structure-based drug design (where the structure of the protein and the protein-ligand complex has been used design better and better inhibitors) suffer from poor bioavailability and nasty toxicity. The bioavailability problem is often associated with poor solubility: good inhibitors often are most “at home” in the mostly hydrophobic environment of a typical enzymatic active site, and so they often have few polar groups on them. Increasing the number of polar groups on the ligand will often improve its solubility by two orders of magnitude or more. The effectiveness of the ligand as an inhibitor will typically be diminished—an inhibitor with  $K_i$  of 10 nM might be changed to one with  $K_i=50$  nM but this is often seen as an acceptable compromise. Increases in solubility will offer less toxicity as well, because the compound is less likely to accumulate as an insoluble mass. But reducing the toxicity of a drug is not necessarily an easy task.

Some molecules retrieved from screening accordingly to Lipinski rule of five have drug like properties. #4 is known as Famotidine and #11 as d-Phe-d-Phe-d-Nle-d-Arg-NH<sub>2</sub> is a well-known peptide sequence with kappa opioid agonist effect respectively [10]. Famotidin interaction with urokinase was predicted successfully value of  $K_i$  found suggesting its pharmacological action and the necessity of its IV administration in urokinase-related anaphylactoid reaction. Having a relatively low affinity for Urokinase (86.339 nM) a higher concentration of this compound is required in the blood stream for Famotidin to achieve therapeutic plasma concentrations. Founding's are in consonance with evidence found in the literature [11].

## Conclusion

ANN was superior in predicting bioactivity compared to multiple linear regressions (MLR). A model with an  $r^2$  of 0.9614 resulted using a library of 42 compounds. The ANN model was used successfully in similarity ranking of the data library. Shape screening retrieved

compounds with drug like properties. ANN model predicted in a realistically domain the  $K_i$  retrieving no errors and no bias values, all the  $K_i$ 's predicted being in the activity range

## References

1. Rockway TW, Nienaber V, Giranda VL (2002) Inhibitors of the protease domain of urokinase-type plasminogen activator, *Curr Pharm Des* 8: 2541-2558.
2. Vaughan DE (2005) “PAI-1 and atherothrombosis”. *Journal of Thrombosis and Haemostasis* 3: 1879-1883.
3. AHFS Drug Information (1992) American Society of Hospital Pharmacists, Bethesda.
4. Jeffrey A Perri, Kurt R Stahfeld, Edward R Villella, Samuel T Simone, Michael E Lally (1994) The management of anaphylactoid reactions to urokinase, *Journal of vascular surgery* 20: 846-847.
5. Chen X, Lin Y and Gilson MK (2002) Overview and User's Guide Biopolymers *Nucleic Acid Sci* 61: 127-141.
6. BehzadEftekhari, Kazem Mohammad, Hassan Eftekhari Ardebili, Mohammad Ghodsi, Ebrahim Ketabchi (2005) Comparison of artificial neural network and logistic regression models for prediction of mortality in head trauma based on initial clinical data, *BMC Med Inform Decis Mak* 5: 3.
7. Knofczynski GT, Mundfrom D (2008) Sample sizes when using multiple linear regression for prediction. *Educational and Psychological Measurement* 68: 431-442.
8. John J Irwin, Brian K Shoichet (2005) ZINC – A Free Database of Commercially Available Compounds for Virtual Screening, *J ChemInf Model* 45: 177-182.
9. Rott O, Olson AJ (2010) “AutoDockVina: Improving the speed and accuracy of docking with a new scoring function, efficient optimization, and multithreading”, *Journal of Computational Chemistry* 31: 455-461.
10. Vanderah TW, Schteingart CD, Trojnar J, Junien JL, Lai J, et al. (2004) FE200041 (D-Phe-D-Phe-D-Nle-D-Arg-NH<sub>2</sub>): A peripheral efficacious kappa opioid agonist with unprecedented selectivity. *J Pharmacol Exp Ther* 310: 326-333.
11. Vidovich RR, Heiselman DE, Hudock D (1992) Treatment of urokinase-related anaphylactoid reaction with intravenous famotidine. *Ann Pharmacother* 26: 782-783.

**Copyright:** ©2018 Claudiu N Lungu. This is an open-access article distributed under the terms of the Creative Commons Attribution License, which permits unrestricted use, distribution, and reproduction in any medium, provided the original author and source are credited.